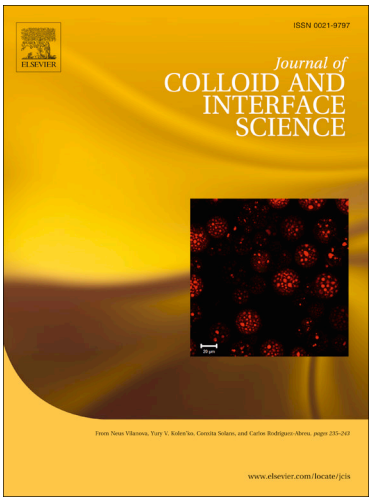

Structure of Surfactant and Phospholipid Monolayers at the Air/Water Interface modeled from Neutron Reflectivity Data

Richard A. Campbell, Yussif Saaka, Yanan Shao, Yuri Gerelli, Robert Cubitt, Ewa Nazaruk, Dorota Matyszewska, M. Jayne Lawrence

PII: S0021-9797(18)30778-1
DOI: https://doi.org/10.1016/j.jcis.2018.07.022
Reference: YJCIS 23813

To appear in: *Journal of Colloid and Interface Science*

Received Date: 31 May 2018
Revised Date: 6 July 2018
Accepted Date: 6 July 2018

Please cite this article as: R.A. Campbell, Y. Saaka, Y. Shao, Y. Gerelli, R. Cubitt, E. Nazaruk, D. Matyszewska, M. Jayne Lawrence, Structure of Surfactant and Phospholipid Monolayers at the Air/Water Interface modeled from Neutron Reflectivity Data, *Journal of Colloid and Interface Science* (2018), doi: https://doi.org/10.1016/j.jcis.2018.07.022

Structure of Surfactant and Phospholipid Monolayers at the Air/Water Interface modeled from Neutron Reflectivity Data.

Richard A. Campbell[1,2], Yussif Saaka[3], Yanan Shao[3], Yuri Gerelli[2], Robert Cubitt[2], Ewa Nazaruk[4], Dorota Matyszewska[5] & M. Jayne Lawrence[1,3]*

1. Division of Pharmacy and Optometry, Faculty of Biology, Medicine and Health, University of Manchester, Stopford Building, Oxford Road, Manchester M13 9PT, United Kingdom

2. Institut Laue-Langevin, 71 avenue des Martyrs, CS20156, 38042 Grenoble, France

3. Institute of Pharmaceutical Sciences. Faculty of Life Sciences and Medicine, King's College London, Franklin-Wilkins Building, Stamford Street, London SE1 9NH, United Kingdom

4. Faculty of Chemistry, University of Warsaw, Pasteura 1, 02-093 Warsaw, Poland

5. Faculty of Chemistry, Biological and Chemical Research Centre, University of Warsaw, Żwirki i Wigury 101, 02-089 Warsaw, Poland

ABSTRACT: Specular neutron reflectometry is a powerful technique to resolve interfacial compositions and structures in soft matter. Surprisingly however, even after several decades, a universal modeling approach for the treatment of data of surfactant and phospholipid monolayers at the air/water interface has not yet been established. To address this shortcoming, first a systematic evaluation of the suitability of different models is presented. The result is a comprehensive validation of an optimum model, which is evidently much needed in the field, and which we recommend as a starting point for future data treatment. While its limitations are openly discussed, consequences of failing to take into account various key aspects are critically examined and the systematic errors quantified. On the basis of this physical framework, we go on to show for the first time that neutron reflectometry can be used to quantify directly *in situ* at the air/water interface the extent of acyl chain compaction of phospholipid monolayers with respect to their phase. The achieved precision of this novel quantification is ~ 10%. These advances together enhance significantly the potential for exploitation in future studies data from a broad range of systems including those involving synthetic polymers, proteins, DNA, nanoparticles and drugs.

Introduction

Specular neutron reflectometry (NR) is an experimental technique that can be used to provide a direct measure of the surface excess of a surfactant or phospholipid monolayer at the air/water interface thanks to the use of isotopic contrast variation.[1,2] It can also be used to reveal the interfacial composition and structure of more complex systems through the application of a common physical model to data recorded in multiple isotopic contrasts. An important reason for the use of isotopic labeling is that deuterium scatters neutrons strongly and in a different phase to hydrogen, so the incorporation of deuterium atoms in a species enhances its sensitivity selectively, and mixtures of H_2O and D_2O can be used to tune the scattering of an aqueous subphase. Recent advances in instrumentation have meant that it is now possible to resolve the surface excess of a single deuterated species on the second time scale and the composition of a binary mixture involving only one deuterated component on the minute time scale.[3,4,5]

Nowadays, NR provides routine insight into complex systems in soft matter and biology.[6,7] It is most common to treat experimental reflectivity data through fitting models using the optical matrix or Parratt formulism for stratified media.[8] Surprisingly, however, the approach to model even a system as simple as a surfactant or phospholipid monolayer at the air/water interface is far from universal. Variations in the approach include whether to account for changing monolayer coverage by varying its thickness or density, which itself appears to be related to the need to include surface roughness, whether to have one or more layers, and whether to account for a change in density of a phospholipid with respect to its phase.

A model where changing coverage is accounted for principally by a change in density rather than thickness, while effects of surface roughness are neglected, appears to date back to an early NR study on Langmuir monolayers of 1,2-dipalmitoyl-sn-glycero-3-phosphocholine (DPPC) in 1994.[9] It was stated that surface roughness was not included in the model as it did not improve the quality of the fits. In work soon after on Gibb's monolayers of sodium dodecylsulfate (SDS) in 1995,[10] the applied model involved a single layer with a thickness close to the all-*trans* conformation of the alkyl chains and different volume fractions. This model, with the molecules standing rigidly on end, was applied even at monolayer coverage of $< 10\%$. While the physical basis of such a model may be reasonably questioned, good agreement with the data, although notably in only one isotopic contrast of the subphase, was demonstrated. Zero[11] or rather low[12] layer roughness values have continued to be used in some studies, and inclusion or not of the parameter in applied models is not even mentioned in others to this day.[13,14] Such an approach may have originated as a result of the lower neutron flux over the accessible range in the momentum transfer normal to the interface, Q_z, on early instruments and/or the assumption that inclusion of roughness in a model is simply a consequence of not having split the system into enough layers.[15]

Such an approach is seemingly in contradiction to the capillary wave roughness of ~ 2.8 Å for a bare air/water interface resulting from thermal fluctuations,[16,17] and its inverse square root dependence on the surface tension

resulting in values of ~ 4 Å for monolayers of the surfactants SDS and dodecyltrimethylammonium bromide (C_{12}TAB).[18] Indeed it was argued in one fairly early study,[19] and is now becoming increasingly common, for layer roughness values whose minimum are consistent with the presence of capillary waves to be applied in models used to fit neutron reflectivity data at fluid interfaces.[20,21] Higher layer roughness values have been used in studies on proteins and nanoparticles[22] or cross-linked polymer nanogels[23] at the air/water interface. Also, in one early study on monolayers of hexadecyltrimethylammonium bromide that exploited kinematic data analysis, it was commented that the air/water interface is even rougher than that predicted from a simple capillary wave model.[24] As such, researchers could be forgiven for forming a general impression from the literature of inconsistency and confusion about what is a reasonable modeling approach to adopt.

Another issue of variation in data modeling approaches is the number of layers required to model data of a surfactant or phospholipid monolayer at the air/water interface. Even recently, neutron reflectivity data recorded of mixtures involving phospholipids were fitted in only one isotopic contrast of the subphase using a 1-layer interfacial model.[25,26] On the other hand, in many other studies the chains and solvated headgroups have been split into separate layers and layer roughness values consistent with the presence of capillary waves were used.[27,28] These studies all aimed to resolve information about effects of interactions on the interfacial structure, yet it has remained unclear to researchers which of the modeling approaches are in fact physically realistic.

A further issue that is not approached universally in the modeling of neutron reflectivity data of phospholipid monolayers is the compaction of acyl chains with respect to their phase.[29] It has been known for decades that the volume of methylene groups reduces by around 4–5 Å^3 from the liquid to crystalline phases,[30] and a recent study has reported an effective reduction of the volume of hydrocarbon chains to be ~ 15%.[31] However, it is unclear if this effect needs to be incorporated in models or if the technique, with its limited accessible Q_z-range,[32] is insensitive to the effect. In one recent study the structure of a phospholipid monolayer was discussed with respect to changing surface pressure over the range 20–50 mN m^{-1},[20] and in another an increase in density of the acyl chains layer with increasing surface pressure was discussed in the context of interactions with other species,[33] yet in both cases chain compaction with changing surface pressure was not considered explicitly. Other studies have also not taken into account this effect,[25,26] while in one study partial compaction of the acyl chains was implied by the parameters used although the effect was not discussed,[34] and in another it was discussed that a better fit to X-ray reflectivity data resulted using a higher density for the acyl chains although the reason was not resolved.[35] There are also studies involving neutron reflectivity data from supported bilayers at the solid/liquid interface in which this effect is either taken into account[36] or not.[37] It is important, therefore, to resolve the importance of this issue for the modeling of neutron reflectivity data from biophysical systems in general.

In the present study, first we scrutinize the validity of 3 models to 3 surfactant or phospholipid monolayers in the fluid phase at the air/water interface. The systems are Gibb's monolayers of SDS and C_{12}TAB at 2 times their critical micelle concentration (CMC) as well as Langmuir monolayers of DPPC in its liquid expanded (LE) phase at a surface pressure of 5 mN m^{-1}. Issues addressed concern the validity of models that account for a change in monolayer coverage by a change in density or thickness, that neglect or account for surface roughness, and that treat the monolayer as 1 or 2 layers. Second, we examine the density of chains required to model data of Langmuir monolayers of phospholipids in the liquid condensed (LC) phase through the study of two additional systems. The first is DPPC at 35 mN m^{-1} as representative of a phospholipid in a highly condensed phase. The second is 1,2-dimyristoyl-sn-glycero-3-phosphoserine (DMPS) at 10 mN m^{-1} as representative of a phospholipid much closer to the mixed LE–LC phase, yet still not on the surface pressure plateau where isotope-specific effects can result in different phases for the hydrogenous and deuterated molecules at the same surface pressure.[38,39] Here we examine the sensitivity of the technique to quantify directly the extent of chain compaction.

Our aims are to describe the basis of a robust physical framework that can be used as a promising starting point to model neutron reflectivity data of Gibb's and Langmuir monolayers at the air/water interface, to examine its strengths and limitations, and to resolve its capability to quantify directly *in situ* the monolayer phase. We feel that description of such a framework may lead to more successful routine exploitation in the future of monolayer data including systems that involve interactions with species such as synthetic polymers,[40] proteins,[41] DNA,[42] nanoparticles[43] or drugs.[44]

Experimental Section

Materials

SDS (Sigma; 99.9%) was recrystallized twice from ethanol and C_{12}TAB (Sigma; 99.9%) was recrystallized twice from acetone; each time solutions were cooled over several hours to maximize the purity. Chain-deuterated SDS (d_{25}-SDS) and C_{12}TAB (d_{25}-C_{12}TAB) were used as supplied by the ISIS Oxford Isotope Facility (Didcot, UK). DPPC, DMPS, chain-deuterated DPPC (d_{62}-DPPC) and chain-deuterated DMPS (d_{54}-DMPS) were used as received from Avanti Polar Lipids (> 99%). Pure water was generated by passing deionized water through a Milli-Q unit (total organic content = 4 ppb; resistivity = 18 mΩ.cm). D_2O (Sigma Aldrich; 99.9%) was used as received.

Sample Preparation

For the NR experiments, the (soluble) SDS and C_{12}TAB samples were prepared in standard adsorption troughs and the (insoluble) DPPC and DMPS monolayers were prepared using a Langmuir trough (insert with 300 cm^2 maximum area; Nima, Coventry, UK). For the adsorbed monolayers, data acquisition commenced within a few minutes after sample preparation due to fast equilibration of the samples. The CMCs for SDS and C_{12}TAB were taken as 8 mM and 15 mM, respectively.[45] For the Langmuir monolayers, the surface pressure sensor was a fresh Wilhelmy plate made of a filter paper. After cleaning the subphase, lipid solution (DPPC in chloroform or DMPS in chloroform:methanol 4:1 v/v; each 1 mg/mL) was spread using a Hamilton microsyringe and the system was left for 15 min for solvent evaporation. The barrier speed during compression was 10 mm/min.

The reported surface pressure/area isotherms were performed using a Langmuir trough (250 cm^2 maximum

area; KSV-Nima, Finland) equipped with hydrophilic barriers. The same experimental approach as above was used. The compression modulus, C_S^{-1},[46] is defined as:

$$C_s^{-1} = -A.\frac{d\pi}{dA} \quad (1)$$

where A is area per molecule, and π is surface pressure. This parameter affords information on the physical state of a monolayer, such as its phase, at a given surface pressure.

The data in this study were recorded at 20–22 ℃.

NR Data Acquisition

Neutron reflectivity measurements were recorded on the FIGARO reflectometer at the Institut Laue-Langevin (Grenoble, France).[3] A chopper pair with a wavelength resolution of 7% dλ/λ was used at incident angles of θ = 0.62° and 3.8°. Measurements were recorded in 4 isotopic contrasts: hydrogenous surfactant/phospholipid (h-surf) or deuterated surfactant/phospholipid (d-surf) with a subphase of pure D_2O or a mixture of 8.1% v/v D_2O in H_2O called air contrast matched water (ACMW) that has a scattering length density of zero. Generous measurement times on the order of 1 h were used to optimize the data quality.

Reflectivity profiles comprise absolute measures of the specular neutron reflectivity, R, with respect to Q_z, which is defined as:

$$Q_z = \frac{4\pi\sin\theta}{\lambda} \quad (2)$$

where π is the numerical value (not surface pressure as in eq. 1) and z is the depth coordinate. The figures are displayed on an $RQ_z^4(Q_z)$ scale to highlight the quality of the fits at high Q_z values. Scattering length density profiles normal to the interface for the different isotopic contrasts are shown as insets to the panels.

The data were reduced using COSMOS.[47] Data of the samples were normalized to a measurement of pure D_2O with fits to the total reflection for the data recorded at θ = 0.62° and a reflectivity model for the data recorded at θ = 3.8°. The latter approach was adopted in order to minimize the introduction of systematic errors in the data recorded at the higher incident angle, which occurs on a level of ~3% in the usual procedure of stitching them to the data from the lower incident angle to achieve good overlap. The background was subtracted from the data by sampling regions on both sides of the specular reflection peak using the area detector. Due to the curvature in the background profile with respect to 2θ, this process is imperfect and depends on the scattering of the subphase, the isotopic contrast, the incident angle, and off-specular scattering from the presence of lateral inhomogenities. Residual background values were used consistently as follows: 2×10^{-7} for d-surf/D_2O and h-surf/D_2O (full Q_z-range), 7×10^{-7} for d-surf/ACMW (full Q_z-range), and 1.5×10^{-6} for h-surf/ACMW (low Q_z-range).

Note that while the h-surf/ACMW data are not particularly sensitive to the different models applied, the reason for their inclusion is that they can be highly sensitive to changes as result of subsequent monolayer interactions. Even in their hydrogenous forms, species such as proteins, synthetic polymers and drugs can have a relatively high scattering length density compared with that of a hydrogenous monolayer, so data from this contrast can help to refine quantification of the amounts of these species in mixed monolayers. Therefore it is important to demonstrate that the optimum model determined also gives good agreement with the data from this contrast. Notwithstanding this point, the data from this weakly reflecting contrast for DMPS monolayers at 10 mN m^{-1} were not used in the global fit due to elevated scattering at low Q_z values and a higher residual background level. These observations are consistent with the presence of lateral domains in a mixed LC–LE state, as discussed below.

NR Data Modeling

The data analysis was performed using the Aurore software.[48] The interfacial material was modeled as one or more uniform stratified layers separated by bulk media (air and solvent). The variables for any given layer are the scattering length density (ρ), thickness (d) and roughness (σ), where for a given species, ρ is equal to its scattering length (b) divided by its molecular volume (M_v). Table S1 in part 1 of the Supporting Information reports the values of b, M_v and ρ of the species featured in the present work. The surface excess (Γ) in moles per unit area of a species in a given layer may then be expressed as:[2]

$$\Gamma = \frac{\rho.d.v_f}{b.N_A} \quad (3)$$

where v_f is its volume fraction in the layer and N_A is Avogadro's number.

The change in ρ across an ideal interface located at z_0 is described as a step function, and the associated roughness is zero. A real interface characterized by finite roughness is described by the $\rho(z)$ profile of the ideal interface modulated by an error function (ERF), where[49]

$$ERF\left(\frac{z-z_0}{\sigma\sqrt{2}}\right) = \frac{2}{\sqrt{\pi}}\int_0^{\frac{z-z_0}{\sigma\sqrt{2}}} e^{-t^2}dt \quad (4)$$

This definition is consistent with the root mean square roughness typically used in real space techniques and with the definition used in the determination of capillary wave roughness.[16,17] For the fluid monolayers in the present work, there is no additional component to the roughness from the shape of the molecules, as may be the case for nanoparticles or proteins, so for simplicity the roughness values for all interfaces were constrained to be equal. Note that each interfacial roughness term is accounted for in the reflectivity calculations in a distinct way from the modulation of the scattering length density profiles. In this case, an exponential term is applied that reduces the reflectance from each interface with increasing Q_z according to the formulism of de Boer.[49]

The MINUIT minimization package[50] used in Aurore provides uncertainty values from evaluation of the variation of χ^2 upon changes in the parameter values, where

$$\chi^2 = \frac{1}{N-N_p}\sum_{i=1}^{N}\frac{\left(R_{exp}(Q_{z,i})-R_{theo}(Q_{z,i})\right)^2}{\varepsilon_i^2} \quad (5)$$

and N is the number of experimental points, N_p is the number of free parameters, R_{exp} and R_{theo} are the experimental and theoretical reflectivity, respectively, and ε_i is the error on the i^{th} experimental point.[52] Reported values of the uncertainties account for any correlation between parameters. Note that χ^2 is a measure of distance between the model curve and the error bars, not the points. Since the values are weighted by the experimental errors, datasets with high counting statistics (i.e. with generous acquisition times and/or on a high flux instru-

ment) will have commensurately low error bars that fail to take into account all of the systematic and random errors in the measurement. In this case, relatively large absolute values of χ^2 will result compared with the application of the same model to datasets with poorer counting statistics. As such, the relative χ^2 values are compared to evaluate the application of different models to the same datasets while we do not discuss the absolute values.

Scheme 1 displays sketches that demonstrate the principles of the 3 models for monolayers of high coverage in terms of the number of layers, and their thickness, density and roughness; the sketches at low coverage simply emphasize further these principles even though such samples are not featured in the present work. The optimum results from these models are presented.

Model 1 has one interfacial layer with a fixed thickness determined by the all-*trans* length of the chains, a single free fitting parameter of the volume fraction of solvent in the layer, and zero layer roughness values. It is similar to the physical model reported in some of the early studies on DPPC[9] and SDS[10] monolayers.

Model 2 also has one interfacial layer but with a fixed volume fraction equal to 1, a single free fitting parameter of the layer thickness, and fixed layer roughness values consistent with the presence of capillary waves.[16,17,18] Here the roughness values are calculated through the inverse square root dependence of the known surface tension for the given sample with respect to the value of ~ 2.8 Å for pure water with ~ 72 mN m^{-1} at room temperature.[53] The roughness values used for monolayers of SDS and C_{12}TAB at 2 times their CMC and DPPC at 5 mN m^{-1} are 4.0, 3.9 and 2.9 Å, respectively.

Model 3 has 2 interfacial layers: layer 1 next to the air containing the chains with a fixed volume fraction equal to 1 and a single free fitting parameter of the thickness, and layer 2 next to and immersed in the solvent containing the headgroups also with a fixed thickness estimated from the molecular dimensions and a constrained volume fraction to respect the molecular structure. The hydrated headgroup layer thickness values used for monolayers of SDS and C_{12}TAB at 2 times their CMC and DPPC at 5 mN m^{-1} are 4.0, 6.0 and 10.0 Å, respectively. Fixed layer roughness values from capillary waves are again used as above. The molecular constraint is implemented by the application of eq. 3 to both the chain and solvated headgroup layers, which we denote with subscripts 1 and 2, respectively, through:

$$\Gamma = \frac{\rho_1.d_1}{b_1.\mathrm{N_A}} = \frac{\rho_2.d_2.v_{f,2}}{b_2.\mathrm{N_A}} \qquad (6)$$

where by approximation $v_{f,1} = 1$, and by rearrangement this gives an equation to calculate the volume fraction of layer 2:

$$v_{f,2} = \frac{\rho_1.d_1.b_2}{\rho_2.d_2.b_1} \qquad (7)$$

The hydration of the headgroups layer is therefore inversely proportional to the surface excess, as calculated directly from the fitted parameter d_1. The standard version of the Aurore software has been developed as part of this work to apply this constraint during a global fit of neutron reflectivity data recorded in multiple isotopic contrasts.[48] In this approach, data in different isotopic contrasts are fitted simultaneously to minimize the overall χ^2 value. This approach relies on the assumption that data in different contrasts have identical chemical structures. It is not currently possible to do this in the standard versions of other programs like RasCAL (https://sourceforge.net/projects/rscl/) or Motofit.[54] This limitation can be circumvented through application of a laborious iterative procedure, however, and a suggested possible workaround to the problem is described in part 2 of the Supporting Information.

In spite of the software development to apply the above constraint during a global fit of data recorded in multiple isotopic contrasts, still it has not yet been possible to perform this procedure while also simultaneously fitting the scattering length density of the acyl chains layer and applying a constraint for the layer to have the same physical density in the different isotopic contrasts. This capability was required for modeling the data of phospholipid monolayers in which extent of acyl chain compaction, $\%C$, was examined, which is defined as

$$\%C = 100 \times \frac{\rho_{\mathrm{appl.}} - \rho_{\mathrm{LE}}}{\rho_{\mathrm{LC}} - \rho_{\mathrm{LE}}} \qquad (8)$$

where $\rho_{\mathrm{appl..}}$ is the applied scattering length density of the acyl chains layer, ρ_{LE} and ρ_{LC} are the calculated values in the LE and LC phases, respectively, and $\rho_{\mathrm{LE}} = 0.85 \times \rho_{\mathrm{LC}}$.[30,31] As a result, Model 3 was applied to data over a discrete range of calculated $\%C$ values, and the optimum model was attributed to the global fit corresponding to the minimum of a resulting $\chi^2(\%C)$ plot. The uncertainty in $\%C$ is ascribed to a single unit increase in the $\chi^2(\%C)$ plot.[48] More details can be found in part 3 of the Supporting Information.

Results

1. Monolayers in the fluid phase

We start by describing the application of different models to neutron reflectivity data of SDS and C_{12}TAB monolayers at 2 times their CMC and DPPC monolayers in the LE phase at 5 mN m^{-1}. Fig. 1 shows data only for the commonly-used isotopic contrast d-surf/ACMW with the application of the 3 different models (Scheme 1). All of the models result in visually satisfactory agreement with the data for SDS and C_{12}TAB. The reason why different models can seem reasonable is that in changing from Model 1 to Models 2 or 3, a reduced thickness makes the model at mid-to-high Q_z higher while inclusion of finite roughness makes it lower. While these effects are not mathematically correlated their effects approximately compensate each other. It may be inferred from these results that the model does not need to be split up into 2 layers. It is clear therefore why if data of a new system are measured in only this isotopic contrast, different types of model could appear to be satisfactory. Even so, Model 1 fails for the data recorded of DPPC across the whole Q_z-range while Model 2 is also poor. These differences demonstrate that the compensation effect between thickness and roughness does not work for the phospholipid with its longer chains, a fact which is related to the position of the minimum of the first Keissig fringe being closer to the accessible measured Q_z-range.

We go on now to examine the application of these models to data recorded in multiple isotopic contrasts in order to evaluate the validity of extracting structural information. As such, the 3 models are applied to data of the 3 systems recorded in 4 isotopic contrasts (d-surf and h-surf each in ACMW and D_2O).

Model 1 is first applied to the data in Fig. 2 with the modeling parameters listed in Table S2 in part 1 of the

Supporting Information. Its agreement with the data is poor for all 3 systems. The model for h-surf/D_2O results in a pronounced Keissig fringe that is not evident in the data for any of the measured systems, and the model for d-surf/D_2O lies above the data at high Q_z. These features demonstrate that the chains of the monolayers are not as extended as their all-*trans* length, and the actual interfacial structure is poorly described by this model.

Model 2 is next applied to the data in Fig. 3 with the modeling parameters listed in Table S3 in part 1 of the Supporting Information. While the agreement is better, still it fails to give satisfactory agreement. For SDS (where the headgroup is relatively small) the agreement fails only marginally for h-surf/D_2O, for C_{12}TAB (with a larger headgroup) the model lies above the data for both h-surf/D_2O and d-surf/D_2O, and for DPPC (with the largest headgroup of the three systems) the agreement for d-surf/D_2O is very poor as there is a Keissig fringe in the data that is not described by the model. These features demonstrate that the interfacial structure is more extended than the model implies. In summary, Models 1 and 2 with only 1 layer are generally insufficient to describe data recorded in multiple isotopic contrasts.

Model 3 is lastly applied to the data in Fig. 4 with the modeling parameters listed in Table S4 in part 1 of the Supporting Information. This model gives the best agreement to the data for all 3 systems: the global χ^2 values for the simultaneous fits in 4 contrasts are better by an average factor of 11 compared with Model 1 and an average factor of 2 compared with Model 2. In order to model the structure of surfactant or phospholipid monolayers in the fluid phase from neutron reflectivity data, therefore, it is advised: (1) to split the chains and solvated headgroups into separate layers, (2) to include layer roughness values consistent with the presence of capillary waves, and (3) to fix the volume fraction of the chains layer to unity.

Note that variations of model 3 were explored as well where either the thickness of the hydrated headgroup layer or the layer roughness values were included as a second fitting parameter. In the former case, the headgroup thickness changed by < 2 Å for C_{12}TAB and DPPC at 5 mN m^{-1}, but the value converged to a physically unrealistic value (< 2 Å) in the case of SDS. At the same time, there was a minimal effect of $< 10\%$ on the χ^2 values. It may be optimal on a case by case basis therefore to test fitting the hydrated headgroup thickness as well to see if physically realistic values are obtained, and if not to constrain it to a value consistent with the molecular dimensions. In the latter case, there were minimal changes to the data or fit quality: the roughness changed by < 1 Å and the χ^2 changed by $< 5\%$. This result confirms that use of physically realistic interfacial roughness in a model is indeed required, and suggests that it may be also left as a free fitting parameter on high quality datasets if so desired.

2. Monolayers in the condensed phase

The optimum modeling approach for neutron reflectivity data of monolayers in the fluid phase (Model 3) is extended now to data of phospholipid monolayers in the LC phase. The scope of this section is to examine data from one phospholipid system in a highly condensed state and another one close to the LE–LC phase boundary. Prior to the consideration of neutron reflectivity data, it is useful to examine surface pressure isotherms of hydrogenous and deuterated samples to help with the choice of systems and critically evaluate the possible impact of isotope-specific effects. One reason for such a comparison is that isotope-specific effects can result in different chemical structures resulting at the same surface pressure due to the different interaction energies associated with H-bonds and D-bonds.[55] This effect can be particular pronounced in affecting the phase of phospholipids (i.e. the shape of a plateau in the surface pressure isotherm) around a phase transition.[38,39]

Fig. 5 shows surface pressure/area isotherms for the phospholipids DPPC and DMPS in their hydrogenous and deuterated forms with compression modulus plots shown in the insets. Both phospholipids undergo an LE–LC phase transition, which is marked by a plateau (or pseudo plateau) in the isotherm and a corresponding minimum in the compression modulus plot. For hydrogenous DPPC, the phase transition begins at ~ 7 mN m^{-1}, and the maximum value of C_S^{-1} is 230 mN m^{-1}, which corresponds to the LC phase.[56] It may be noted that the plateau in the surface pressure isotherm increases in magnitude with increasing temperature,[57] and in fig. 5 lies at an intermediate value compared with those observed in literature measurements recorded at lower (e.g. ~ 5 mN m^{-1})[58,59] and higher (e.g. ~ 10 mN m^{-1})[60] temperatures. For hydrogenous DMPS, the phase transition occurs at lower surface pressures (~ 4 mN m^{-1}) compared to DPPC, and further compression leads to the formation of a highly condensed monolayer as shown by the higher maximum value of C_S^{-1} of 450 mN m^{-1}.[61]

The hydrogenous and deuterated analogues of both phospholipid systems exhibit differences in their surface pressure isotherms around the phase transitions, which is attributed to isotope-specific effects resulting from differences in the chain melting temperatures.[39,62] It is beneficial to choose systems to study at surface pressures that do not result in very different phases for the isotopic analogues. Nevertheless, small differences in the extent of acyl chain compaction close to the phase transition are an inevitable feature of phospholipid systems. Importantly, it is the data from the two contrasts involving deuterated phospholipid that have the most sensitivity to the monolayer phase, as can be seen below (cf. Figs 6A vs. 6B, for example), so the impact on the global fit of small deviations in the phase of hydrogenous and deuterated phospholipids is minor.

On the basis of these complementary data, we chose to study monolayers of DPPC at 35 mN m^{-1}, which are in a highly condensed state far from the phase transition, and DMPS at 10 mN m^{-1}, which are much closer to but just past the phase transition. In the latter case, it is important to note that while the phase of the hydrogenous and deuterated phospholipids are not identical, the chosen surface pressure does fall after the phase transition (i.e. the minimum the compression modulus plot) in both cases. Neutron reflectivity data and models are shown in Fig. 6 with the modeling parameters listed in Table S5 in part 1 of the Supporting Information.

In order to examine the relevance of inclusion of compaction of acyl chains with respect to its phase in models of neutron reflectivity data of phospholipid monolayers, Model 3 is first applied to data of DPPC monolayers at 35 mN m^{-1} recorded in 4 isotopic contrasts while keeping the scattering length density of the acyl chains the same as that in the LE phase. Fig. 6A shows that the models for

d-surf/ACMW and d-surf/D_2O do not describe well the data. Now we consider specific interactions resulting from the transition of chains to the LC phase, given that their volume reduce by ~ 15%,[30,31] and their scattering length density therefore increases commensurately. Models were applied for a discrete range of physical densities and the minimum value of the χ^2, reported in part 3 the Supporting Information, was used to determine the optimum fit. Fig. 6B shows the result in which the model matches the data recorded in all 4 contrasts. The value of $\%C$ is 90 ± 11, which is accompanied by a global χ^2 value that is better by a factor of > 4. The high value of $\%C$ is supported qualitatively by measured values of C_S^{-1}, which although still in the LC phase are very close to the border value of the solid phase at 250 mN m^{-1}.[56] The observation is also backed up by data from polarization modulation-infrared reflection absorption spectroscopy (PM-IRRAS) obtained for DPPC monolayers at 30 mN m^{-1} where the relative low wavenumbers of the CH_2 stretches indicate an increase in *trans* conformations.[63] This result alone demonstrates that the phase of a phospholipid monolayer needs to be taken into account in models used to treat neutron reflectivity data.

It is worth highlighting that the layer roughness values do not increase monotonically with higher capillary waves for DPPC monolayers in the LC phase due to the higher bending stiffness of acyl chains in the condensed phase, which damps thermal fluctuations.[9,64] As the two effects can roughly compensate each other, the layer roughness values used in the model were simply kept the same as in the LE phase. This result implies that if one fixes rather than fits the roughness values for lipid monolayers, awareness of its phase at the given surface pressure is necessary.

Fig. 6C shows the application of Model 3 to neutron reflectivity data of DMPS monolayers at 10 mN m^{-1}. In this case the value of $\%C$ is 56 ± 10. The phase of the monolayer is therefore only about half as condensed as DPPC at 35 mN m^{-1}, which follows given that islands of condensed domains of PS lipids form at low surface pressures.[57] Note that the weakly reflecting h-surf/ACMW data were discarded from this global fit in this case due to increased scattering at low Q_z values and a higher residual background. These features are both attributed to the presence of condensed domains in the monolayer, a point which is elaborated in part 4 the Supporting Information.

In summary, these determinations of the extent of acyl chain compaction in phospholipid monolayers using NR result in qualitatively reasonable values on the basis of indirect indications from complementary techniques. This is the first time that the phase of different lipid monolayer systems has been directly quantified *in situ* at the air/water interface to the best of our knowledge.

Discussion

The framework set out above to model neutron reflectivity data of surfactant and phospholipid monolayers has been shown to work for data recorded in 4 isotopic contrasts for 5 systems involving (soluble) Gibb's monolayers and (insoluble) Langmuir monolayers in different phases. There can be serious consequences on the quality of the fits to data recorded in different contrasts and the accuracy of structural information extracted if key criteria of the framework are not respected, e.g., application of a model with only a single interfacial layer, mixing of air or solvent into the chains layer, neglect of surface roughness or failure to account for the monolayer phase. Interestingly, however, it was shown that such an approach does not always result in serious consequences on the quality of the fits in every contrast. The implication is that if data are modeled only in a reduced number of contrasts (and in some cases only one) then a structural model may appear to be valid even though it would not in fact be supported by fits to data in other contrasts. As such, it is apparent that the structural parameters reported in many literature studies contain significant systematic errors.

Satisfactory agreement to data of monolayers with C_{12}-chains can result for d-surf/ACMW with Model 1, which neglects surface roughness and has a reduced monolayer density (effects that approximately counteract each other). Such a result may imply that the monolayer thickness remains close to the all-*trans* length of the molecule even at low coverage. In addition to the lack of physical reality of this model, its application to data recorded in different isotopic contrasts is not supported for any of the systems in the present work. Furthermore, there is no evidence from the present work, to the resolution of the applied technique, that mixing of air into the chains layer improves the structural characterization of any of the surfactant or phospholipid systems at high coverage studied. It appears that such models may have been applied historically as a consequence of neglect (or under-estimation) of the surface roughness, the effects of which approximately compensate each other (in certain isotopic contrasts). If we scrutinize the thicknesses of the layer in Model 1, we can see for the 3 systems studied that they are 20–40% too large compared with the total monolayer thicknesses determined using the robust Model 3.

The necessity to split the monolayer into 2 layers, one for the chains and one for the solvated headgroups, was demonstrated for data recorded in multiple isotopic contrasts even when surface roughness is taken into account. This aspect of the model was required for satisfactory fits to data recorded in D_2O for all of the systems studied, and also for d-surf/ACMW of the phospholipid with its C_{16}-chains. This result raises a question concerning implications of the use of a 1-layer model to extract structural information only from d-surf/ACMW data. In such a case, the scattering is dominated by the interaction of neutrons with the deuterated chains of the monolayer, so it follows that the total interfacial thickness will be underestimated. If we scrutinize the thickness of the monolayers in Model 2, we can see for the 3 systems studied that they are 20–25% too small compared with the total monolayer thicknesses determined using the robust Model 3.

These findings imply that it may be appropriate to re-evaluate some of the conclusions drawn in studies where unsupported modeling approaches have been used.

We turn now to the issue of the phase of monolayers at the air/water interface. Compaction of acyl chains in phospholipid monolayers with respect to their phase has not been generally incorporated in models of neutron reflectivity data. Further, while it is known that that the modeling of data in multiple isotopic contrasts improves the effective resolution of the NR technique, it is commonly assumed that if the signal cannot be resolved above the background to a Q_z-value of $2\pi/d$, which

marks the minimum of the first Keissig fringe (e.g., 0.4 Å^{-2} for DPPC monolayers at 35 mN m^{-1}), it is not possible to resolve ρ and d independently but instead only their product.[39] A question was open therefore about whether or not it is necessary to take acyl chain compaction into account in such models. In the present work, even though the maximum value of Q_z was resolved only to around half of $2\pi/d$, we have shown that it is necessary to take into account the extent of acyl chain compaction in models of neutron reflectivity data of monolayers at the air/water interface, and further that it is in fact possible to quantify to a precision of ~ 10% the density of the acyl chains (i.e. ~ 15 Å^3 in volume) independently of the thickness.

Information on the compaction of acyl chains of phospholipid layers may also be obtained by spectroscopic techniques such as PM-IRRAS.[65] It has been shown that the tilt angles are smaller for DMPS compared to DMPC, which suggests that DMPS molecules are more closely packed due to different headgroups interactions. Information has also been provided on the chain ordering and the phase of phospholipid bilayers as the position of CH_2 stretching bands can be related to the presence of gauche defects and chain melting.[66] These general rules were later extended to phospholipid monolayers.[67] Nevertheless, the present work marks the first time to our knowledge that NR has been used to quantify directly the extent of this effect at the air/water interface with respect to the monolayer phase. The significance of this result lies in the fact that phase transitions occur in lipid systems not only as a function of the surface pressure but also ionic strength,[58] pH[59] and temperature.[68] Therefore the implications of this result may extend to a broad range of different studies.

It is interesting to note that in an early NR study on DPPC monolayers, data from 2 isotopic contrasts were modeled using a 2-layer interfacial model without surface roughness, and it was concluded that the headgroup thickness is reduced with increasing surface pressure.[69] In the application of the robust model to neutron reflectivity data recorded in 4 isotopic contrasts validated in the present work, we have found no evidence for this effect. Although the thickness of hydrated headgroups layer was fixed at 10 Å according to the molecular dimensions for the data both at 5 and 35 mN m^{-1}, free fitting of this parameter as well resulted in minimal changes (< 1 Å), and the thickness of the layer was in fact very slightly higher (~1 Å) at the higher surface pressure. The lack of significant changes in the structure of the headgroup region was also discussed in a Fourier transform infrared spectroscopy study of oriented phospholipid multilayers, as the spectra corresponding to C=O bands recorded for hydrated films both below and above the phase transition temperature were similar.[70]

Regarding another misconception in neutron reflectivity data analysis, it is commonly assumed that it is unacceptable to apply roughness values in a multilayer slab model that exceed around one third of the thickness of any adjacent layer. However, it is not universally appreciated that it is only the asymmetric application of different roughness values at the interfaces that bind a given layer that can result in a physically unrealistic scattering length density profile, i.e., a region can contain a negative amount of a component. This problem is not suffered if the respective layer roughness values applied are the same, which is the case in the robust model described in the present work. The consequence of relatively large roughness values in its application is broadening of the density profile with the maximum density not reaching that of the pure component in the layer. However, it can be demonstrated that reflectivity calculations accurately quantify the amount of material (i.e. the integration of scattering length density and distance) even if the roughness values match that of the layer thickness. These points are discussed further in part 5 the Supporting Information. Therefore we can conclude that the robust model is physically valid even though (1) the layers are rather thin as the chains and hydrated headgroups are separated into different layers and the density in the former case is not reduced with decreasing coverage, and (2) roughness values that are consistent with the existence of capillary waves are applied.

Lastly, we comment on our observations that the optimum model described in the present work does fail in certain cases. First, we have observed for d_{75}-DPPC monolayers, the model drops below the data in the d-surf/D_2O contrast. This effect is attributed to the specific detailed structure of the headgroup: deuterium atoms are located at its tip, so effectively there is a minimum in the scattering length density profile at the start of the headgroup (next to the chains), which is not accounted for if the solvated headgroups are modeled as a single layer. As a result, for simplicity, we suggest that d_{62}-DPPC may be generally preferable as the deuterated analogue of choice over d_{75}-DPPC for many structural studies using NR. Second, we have also observed that the model also does not match well data from SDS samples if the purity of the samples is poor. The presence of dodecanol results in deviations of the model at mid-to-high Q_z values to data involving the 2 contrasts in D_2O. We recommend that if such deviations are observed greater attention should be paid to purification of the samples.

Conclusions & Outlook

In the present work, we have thoroughly validated a robust model for fitting neutron reflectivity data recorded in multiple isotopic contrasts of surfactant and phospholipid monolayers at the air/water interface. Key features of the model include the splitting the molecules into separate layers for the chains and solvated headgroups, inclusion of surface roughness consistent with the presence of capillary waves, fixing the volume fraction of the chains to unity, and taking into account the monolayer phase. The model has just one free fitting parameter although fitting the hydrated headgroup layer thickness as well was reasonable in certain cases and fitting the layer roughness values was reasonable in every case. Strengths and limitations of this model as a promising starting point to fit monolayer data of new systems in the future have been discussed.

Approaches used in various structural studies in the literature have neglected some or all of these features and/or have involved fitting data recorded in fewer isotopic contrasts and in cases only one.[e.g. 9,10,11,13,14,25,26] In the case of a deuterated surfactant or phospholipid in air contrast matched water, structural implications of the model deviate significantly from the physical picture that is supported by the validated robust model. It has been shown that in cases where structural details are interpreted explicitly, a single-layer interfacial model without surface roughness may over-estimate the mono-

layer thickness by around one third, while a single-layer model with surface roughness may under-estimate the thickness by around one quarter.

Another focus of this work was to examine if NR can be used to quantify the extent of acyl chain compaction of phospholipid monolayers with respect to their phase. This effect has not usually been considered explicitly in models used in studies at the air/water interface.[e.g. 20,33,34] We have shown that the effect needs to be taken into account in the modeling of such data at the air/water interface, and we went on to quantify directly its magnitude using NR for the first time in two different systems. This result may be surprising to many who may assume that the technique cannot be used to distinguish density, thickness and roughness as a result of its limited accessible Q_z-range. However, application of the validated robust model to data recorded in multiple isotopic contrasts was shown to be sufficient to overcome this limitation and quantify the monolayer phase directly *in situ* to a precision of ~ 10%. As a result of this advance therefore, it may be possible in the future to gain sharper insight into biophysical processes by resolving the phase of monolayers during or as a result of molecular interactions with a range of systems includeing those involving interactions with synthetic polymers,[40] proteins,[41] DNA,[42] nanoparticles[43] or drugs.[44]. This possibility is of importance given that phase transitions occur as a result of changes in the ionic strength,[58] pH[59] and temperature[68] as well as surface pressure.[57,60]

Lastly, we comment that over the years there has surely been a huge quantity of neutron reflectivity data generated at facilities worldwide that have not been exploited because reasonable agreement with a physical model could not be achieved. The situation may have been exacerbated by the fact that a variety of models applied to data in a limited number of isotopic contrasts in the literature fail to describe data recorded in other isotopic contrasts, so a satisfactory outcome could not be obtained when similar approaches were attempted on new systems. On the basis of the modeling framework described in the present work, not only is it possible to formulate new questions concerning interfacial mechanisms in a broad range of systems in the future, but also revisit previously unexploited data in order to access the information desired originally.

AUTHOR INFORMATION

* Corresponding author: Richard A. Campbell;
richard.campbell@manchester.ac.uk; +44 161 275 7844.

SUPPORTING INFORMATION

Supporting information is available: (1) tables of parameters used in/extracted from NR models; (2) suggested procedure to work around software limitations; (3) extent of acyl chain compaction in phospholipid monolayers; (4) off-specular scattering from domains in DMPS monolayers; (5) conservation of material in models with high interfacial roughness.

ACKNOWLEDGMENTS

We thank the Institut Laue-Langevin for allocations of neutron beam time on FIGARO (DOIs: 10.5291/ILL-DATA.9-10-1348, 10.5291/ILL-DATA.9-10-1465 and 10.5291/ILL-DATA.9-13-683), the ISIS Oxford Isotope Facility for provision of the deuterated surfactants, Jian Lu, Andrew Nelson, Emanuel Schneck, Ernesto Scoppola, Giovanna Fragneto and Tommy Nylander for helpful discussions, Imre Varga and Bence Feher for sample preparation in preliminary experiments, Elżbieta Jabłonowska for recording complementary surface pressure isotherms, and Reneta Bilewicz for involvement in some neutron reflectometry experiments. YSa is thankful for the GETFund research grant. EN and DM thank the support from a SNF Sinergia grant No. CRSII2 154451.

REFERENCES

1. Zhou, X-L.; Chen, S-H. Theoretical foundation of X-ray and neutron reflectometry. *Phys. Rep.* **1995**, *257*, 223–348.

2. Lu, J. R.; Thomas, R. K.; Penfold, J. Surfactant layers at the air-water interface: structure and composition. *Adv. Colloid Interface Sci.* **2000**, *84*, 143–304.

3. Campbell, R. A.; Wacklin, H. P.; Sutton, I.; Cubitt, R.; Fragneto, G. FIGARO: the new horizontal neutron reflectometer at the ILL. *Eur. Phys. J. Plus* **2011**, *126*, 107.

4. Campbell, R. A.; Tummino, A.; Noskov, B. A.; Varga, I. Polyelectrolyte/surfactant films spread from neutral aggregates. *Soft Matter* **2016**, *12*, 5304–5312.

5. Campbell, R. A. Recent advances in resolving kinetic and dynamic processes at the air/water interface using specular neutron reflectometry. *Curr. Opin. Colloid Interface Sci.* **2018**, *37*, 49–60.

6. Narayanan, T.; Wacklin, H.; Konovalov, O.; Lund, R. Recent applications of synchrotron radiation and neutrons in the study of soft matter. *Crystallogr. Rev.* **2017**, *23*, 160–226.

7. Braun, L.; Uhlig, M.; von Klitzing, R.; Campbell, R. A. Polymers and surfactants at fluid interfaces measured with specular neutron reflectometry. *Adv. Colloid Interface Sci.* **2017**, *247*, 130–148.

8. Parratt, L. G. Surface studies of solids by total reflection of X-rays. *Phys. Rev.* **1954**, *95*, 359–369.

9. Brumm, T.; Naumann, C.; Sackmann, E.; Rennie, A. R.; Thomas, R. K.; Kanellas, D.; Penfold, J.; Bayerl, T. M. Conformational changes of the lecithin headgroup in monolayers at the air/water interface. *Eur. Biophys. J.* **1994**, *23*, 289–295.

10. Lu, J. R.; Purcell, I. P.; Lee, E. M.; Simister, E. A.; Thomas, R. K.; Rennie, A. R.; Penfold, J. The composition and structure of sodium dodecyl sulfate-dodecanol mixtures adsorbed at the air-water interface: a neutron reflection study. *J. Colloid Interface Sci.* **1995**, *174*, 441–455.

11. Zarbakhsh, A.; Campana, M.; Webster, J. R. P.; Wojciechowski, K. Stabilization of alkylated azacrown ether by fatty acid at the air-water interface. *Langmuir* **2010**, *26*, 18194–18198.

12. Ciumac, D.; Campbell, R. A.; Xu, H.; Clifton, L. A.; Hughes, A. V.; Webster, J. R. P.; Lu, J. R. Implications of lipid monolayer charge characteristics on their selective interactions with a short antimicrobial peptide. *Colloids Surf. B* **2017**, *150*, 308–316.

13. Bradbury, R.; Penfold, J.; Thomas R. K.; Tucker, I. M.; Petkov, J. T.; Jones, C. Manipulating perfume delivery to the interface using polymer–surfactant interactions. *J. Colloid Interface Sci.* **2016**, *466*, 220–226

14. Xu, H.; Li, P.; Ma, K.; Welbourn, R. J. L.; Doutch, J.; Penfold, J.; Thoma, R. K.; Roberts, D. W.; Petkov, J. T.; Choo, K. L.; Khoo, S. Y. Adsorption and self-assembly in methyl ester sulfonate surfactants, their eutectic mixtures and the role of electrolyte. *J. Colloid Interface Sci.* **2018**, *516*, 456–465.

15. Jia, D.; Tao, K.; Wang, J.; Wang, C.; Zhao, X.; Yaseen, M.; Xu, H.; Que, G.; Webster, J. R. P.; Lu, J. R. Dynamic adsorption and structure of interfacial bilayers adsorbed from lipopeptide surfactants at the hydrophilic silicon/water interface: effect of the headgroup length. *Langmuir* **2011**, *27*, 8798–8809.

16. Braslau, A.; Deutsch, M.; Pershan, P. S.; Weiss, A. H.; Als-Nielsen, J.; Bohr J. Surface roughness of water measured by x-ray reflectivity. *Phys. Rev. Lett.* **1985**, *54*, 114–117.

17. Sinha, S. K.; Sirota, E. B.; Garoff, S.; Stanley, H. B. X-ray and neutron scattering from rough surfaces. *Phys. Rev. B* **1988**, *38*, 2297–2311.

18. Tikhonov, A. M.; Mitrinovic, D. M.; Li, M.; Huang, Z.; Schlossman, M. L. An X-ray reflectivity study of the water-docosane interface *J. Phys. Chem. B* **2000**, *104*, 6336–6339.

19. Lu, J. R.; Ottewill, R. H.; Rennie, A. R. Adsorption of ammonium perfluorooctanoate at the air–water interface. *Colloids Surf. A* **2001**, *183–185*, 15–26.

20. Hollinshead, C. M.; Harvey, R. D.; Barlow, D. J.; Webster, J. R. P.; Hughes, A. V.; Weston, A.; Lawrence, M. J. Effects of surface pressure on the structure of distearoylphosphatidylcholine monolayers formed at the air/water interface. *Langmuir* **2009**, *25*, 4070–4077.

21. Jagalski, V.; Barker, R.; Topgaard, D.; Günther-Pomorski, T.; Hamberger, B.; Cárdenas, M. Biophysical study of resin acid effects on phospholipid membrane structure and properties. *Biochim. Biophys. Acta, Biomembr.* **2016**, *1858*, 2827–2838.

22. Ang, J. C.; Henderson, M.; Campbell, R. A.; Lin, J. M.; Yaron, P. N.; Nelson, A.; Faunce, T. A.; White J. W. Human serum albumin binding to silica nanoparticles - effect of protein fatty acid ligand. *Phys. Chem. Chem. Phys.* **2014**, *16*, 10157–10168.

23. Zielinska, K.; Sun, H.; Campbell, R. A.; Zarbakhsh, A.; Resmini, M. Smart nanogels at the air/water interface: structural studies by neutron reflectivity. *Nanoscale* **2016**, *8*, 4951–5960.

24. Lu, J. R.; Hromadova, M.; Simister, E. A.; Thomas, R. K.; Penfold, J. Neutron reflection from hexadecyltrimethylammonium bromide adsorbed at the air/liquid interface: the variation of the hydrocarbon chain distribution with surface concentration. *J. Phys. Chem.* **1994**, *98*, 11519–11526.

25. Wojciechowski, K.; Orczyk, M.; Gutberlet, T.; Geue, T. Complexation of phospholipids and cholesterol by triterpenic saponins in bulk and in monolayers. *Biochim. Biophys. Acta, Biomembr.* **2016**, *1858*, 363–373.

26. Wojciechowski, K.; Orczyk, M.; Gutberlet, T.; Brezesinski, G.; Geue, T.; Fontaine, P. On the interaction between digitonin and cholesterol in Langmuir monolayers. *Langmuir* **2016**, *32*, 9064–9073

27. Foglia, F.; Fragneto, G.; Clifton, L. A.; Lawrence, M. J.; Barlow, D. J. Interaction of Amphotericin B with Lipid Monolayers. *Langmuir* **2014**, *30*, 9147–9156.

28. Bello, G.; Bodin, A.; Lawrence, M. J.; Barlow, D.; Mason, A. J.; Barker, R. D.; Harvey, R. D. The influence of rough lipopolysaccharide structure on molecular interactions with mammalian antimicrobial peptides, *Biochim. Biophys. Acta, Biomembr.* **2016**, *1858*, 197–209.

29. McConlogue, C. W.; Vanderlick, T. K. A close look at domain formation in DPPC monolayers. *Langmuir* **1997**, *13*, 7158–7164.

30. Small, D. M. Lateral chain packing in lipids and membranes. *J. Lipid Research* **1984**, *25*, 1490–1500.

31. Marsh, D. Molecular volumes of phospholipids and glycolipids in membranes. *Chem. Phys. Lipids* **2010**, *163*, 667–677.

32. Smigiel, E.; Cornet, A. Characterization of a layer stack by wavelet analysis on x-ray reflectivity data. *J. Phys. D: Appl. Phys.* **2000**, *33*, 1757–1763.

33. Bauer, M.; Charitat, T.; Fajolles, C.; Fragneto, G.; Daillant, J. Insertion properties of cholesteryl cyclodextrins in phospholipid membranes: a molecular study. *Soft Matter* **2012**, *8*, 942–953.

34. Dabkowska, A. P.; Collins, L. E.; Barlow, D. J.; Barker, R.; McLain, S. E.; Lawrence, M. J.; Lorenz, C. D. Modulation of dipalmitoylphosphatidylcholine monolayers by dimethyl sulfoxide. *Langmuir* **2014**, *30*, 8803–8811.

35. Dabkowska, A. P.; Talbot, J. P.; Cavalcanti, L.; Webster, J. R. P.; Nelson, A.; Barlow, D. J.; Fragneto, G.; Lawrence, M. J. Calcium mediated interaction of calf-thymus DNA with monolayers of distearoylphosphatidylcholine: a neutron and X-ray reflectivity study. *Soft Matter* **2015**, *9*, 7095–7105.

36. Gerelli, Y.; Porcar, L.; Fragneto, G. Lipid rearrangement in DSPC/DMPC bilayers: a neutron reflectometry study. *Langmuir* **2012**, *28*, 15922–15928.

37. Schenck, E.; Berts, I.; Halperin, A.; Daillant, J.; Fragneto, G. Neutron reflectometry from poly (ethylene-glycol) brushes binding anti-PEG antibodies: evidence of ternary adsorption. *Biomaterials* **2015**, *46*, 95–104.

38. Angus-Smyth, A.; Campbell, R. A.; Bain, C. D. Dynamic adsorption of weakly interacting polymer/surfactant mixtures at the air/water interface. *Langmuir* **2012**, *28*, 12479–12492.

39. Baldyga, D. D.; Dluhy, R. A. On the use of deuterated phospholipids for infrared spectroscopic studies of monomolecular films: a thermodynamic analysis of single and binary component phospholipid monolayers. *Chem. Phys. Lipids* **1998**, *96*, 81–97.

40. Madrid, E.; Horswell, S. L. Effect of deuteration on phase behavior of supported phospholipid bilayers: a spectroelectrochemical study. *Langmuir* **2015**, *31*, 12544–12551.

41. Perriman, A. W.; Henderson, M. J.; Evenhuis, C. R.; McGillivray, D. J.; White, J. W. Effect of the air-water interface on the structure of lysozyme in the presence of guanidinium chloride. *J. Phys. Chem. B* **2008**, *112*, 9532–9539.

42. Dabkowska, A. P.; Barlow, D. J.; Campbell, R. A.; Hughes, A. V.; Quinn, P. J.; Lawrence, M. J. Effect of helper lipids on the interaction of DNA with cationic lipid monolayers studied by specular neutron reflection. *Biomacromolecules* **2012**, *13*, 2391–2401.

43. Reguera, J.; Ponomarev, E.; Geue, T.; Stellacci, F.; Bresme, F.; Moglianetti, M. Contact angle and adsorption energies of nanoparticles at the air-liquid interface determined by neutron reflectivity and molecular dynamics. *Nanoscale* **2015**, *7*, 5665–5673.

44. Saaka, Y.; Allen, D. T.; Luangwitchajaroen, Y.; Shao, Y.; Campbell, R. A.; Lorenz, C. D.; Lawrence, M. J. Towards optimised drug delivery: structure and composition of testosterone enanthate in sodium dodecyl sulfate monolayers. *Soft Matter* **2018**, *14*, 3135–3150.

45. Ábraham, Á.; Campbell, R. A.; Varga, I. New method to predict the surface tension of complex synthetic and biological polyelectrolyte/surfactant mixtures. *Langmuir* **2013**, *29*, 11554–11559.

46. Gaines Jr., G. L. Insoluble monolayers at liquid-gas interfaces. Interscience, New York, 1966, p. 24.

47. Gutfreund, P.; Saerbeack, T.; Gonzalez, M. A.; Pellegrini, E.; Laver, M.; Dewhurst, C.; Cubitt, R. Towards generalized data reduction on a chopper-based time-of-flight neutron reflectometer. *J. Appl. Crystallogr.* **2018**, *51*, 606–615.

48. Gerelli, Y. Aurore: New Software for Neutron Reflectivity Data Analysis. *J. Appl. Cryst.* **2016**, *49*, 330–339.

49. Bhushan, B. "2. Surface roughness analysis and measurement techniques" in "Modern Tribology Handbook". CRC Press, 2000.

50. de Boer, D. K. G. Influence of the roughness profile on the specular reflectivity of x rays and neutrons. *Phys. Rev. B* **1994**, *49*, 5817–5820.

51. James, F. MINUIT function minimization and error analysis. CERN, 1998.

52. Cochran, W. G. The $\chi 2$ test of goodness of fit. *Ann. Math. Statist.* **1952**, *23*, 315–345.

53. Pallas, N. R.; Harrison, T. An automated drop shape apparatus and the surface tension of pure water. *Colloids and Surfaces* **1990**, *43*, 169–194.

54. Nelson, A. Co-refinement of multiple-contrast neutron/X-ray reflectivity data using MOTOFIT. *J. Appl. Crystallogr.* **2006**, *39*, 273–276.

55. Grimison, A. The deuterium isotope effect in the hydrogen bonding of imisazole in naphthalene solutions. *J. Phys. Chem.* **1963**, *67*, 962–964.

56. Harkins, W. D. The physical chemistry of surface films. Reinhold, New York, 1952, p. 107.

57. Minones Jr, J.; Rodriguez Patino, J. M.; Conde, O.; Carrera, C.; Seoane, R. The effect of polar groups on structural characteristics of phospholipid monolayers spread at the air–water interface. *Colloids Surf. A* **2002**, *203*, 273–286.

58. Shapovalov, V. L. Interaction of DPPC monolayer at air–water interface with hydrophobic ions. *Thin Solid Films* **1998**, *327–329*, 599–602.

59. Dahmen-Levison, U.; Brezesinski, G.; Möhwald, H. Specific adsorption of PLA2 at monolayers. *Thin Solid Films* **1998**, *327–329*, 616–620.

60. Zhao, J.; Vollhardt, D.; Brezesinski, G.; Siegel, S.; Wu, W.; Li, J. B.; Miller, R. Effect of protein penetration into phospholipid monolayers: morphology and structure. *Colloids Surf. A* **2000**, *171*, 175–184.

61. Sautrey, G.; Orlof, M.; Korchowiec, B.; Regnouf de Vains, J.-B.; Rogalska, E. Membrane activity of tetra-p-guanidinoethylcalix[4]arene as a possible reason for its antibacterial properties. *J. Phys. Chem. B* **2011**, *115*, 15002–15012.

62. Petersen, N. O.; Kroon, P. A.; Kainosho, M.; Chan, S. I. Thermal phase transitions in deuterated lecithin bilayers. *Chem. Phys. Lipids* **1975**, *14*, 343–349.

63. Aroti, A.; Leontidis, E.; Maltseva,E.; Brezesinski, G. Effects of Hofmeister anions on DPPC Langmuir monolayers at the air–water interface. *J. Phys. Chem. B* **2004**, *108*, 15238–15245.

64. Daillant, J.; Bosio, L.; Benattar, J. J. Meunier, J. Capillary waves and bending elasticity of monolayers on water studied by X-ray reflectivity as a function of surface pressure. *Europhys. Lett.* **1989**, *8*, 453–458.

65. Madrid, E.; Horswell, S. L. Effect of electric field on structure and dynamics of bilayers formed from anionic phospholipids. *Electrochim. Acta* **2014**, *146*, 850–860.

66. Zawisza, I.; Bin, X.; Lipkowski, J. Potential-driven structural changes in Langmuir-Blodgett DMPC bilayers determined by in situ spectroelectrochemical PM IRRAS. *Langmuir* **2007**, *23*, 5180–5194.

67. Schulte, W.; Orlof, M.; Brand, I.; Korchowiec, B.; Rogalska, E. A. Langmuir monolayer study of the action of phospholipase A2 on model phospholipid and mixed phospholipid-GM1ganglioside membranes. *Colloids Surf. B* **2014**, *116*, 389–395.

68. Chou, T-H.; Chang, C-H. Thermodynamic characteristics of mixed DPPC/DHDP monolayers on water and phosphate buffer subphases. *Langmuir* **2000**, *16*, 3385–3390.

69. Bayerl, T. M.; Thomas, R. K.; Penfold, J.; Rennie, A.; Sackmann, E. Specular reflection of neutrons at phospholipid monolayers: changes of monolayer structure and headgroup hydration at the transition from the expanded to the condensed phase state. *Biophys. J.* **1990**, 57, 1095–1098.

70. Hubner, W.; Mantsch, H. H. Orientation of specifically 13C=O labeled phosphatidylcholine multilayers from polarized attenuated total reflection FT-IR spectroscopy. *Biophys. J.* **1991**, 59, 1261–1272.

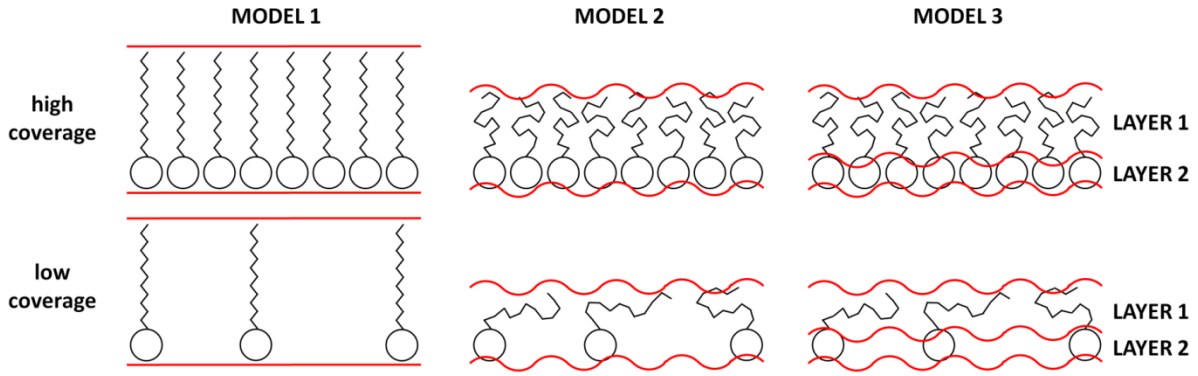

Scheme 1. Sketches of the 3 different models applied in this work to illustrate their key features in the cases of relatively high and low monolayer coverage.

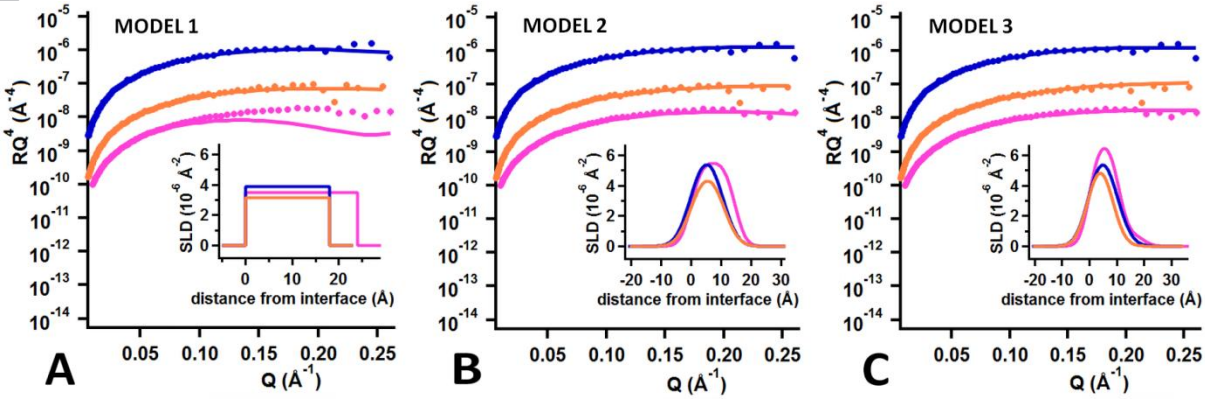

Figure 1. Neutron reflectivity data of monolayers of (dark blue) SDS and (orange) C_{12}TAB at 2 times their CMCs, and (pink) DPPC at 5 mN m^{-1}, recorded in d-surf/ACMW: applications of (A) Model 1, (B) Model 2 and (C) Model 3. For clarity, the data and fits have been offset vertically by increased factors of 100 for SDS and 10 for C_{12}TAB.

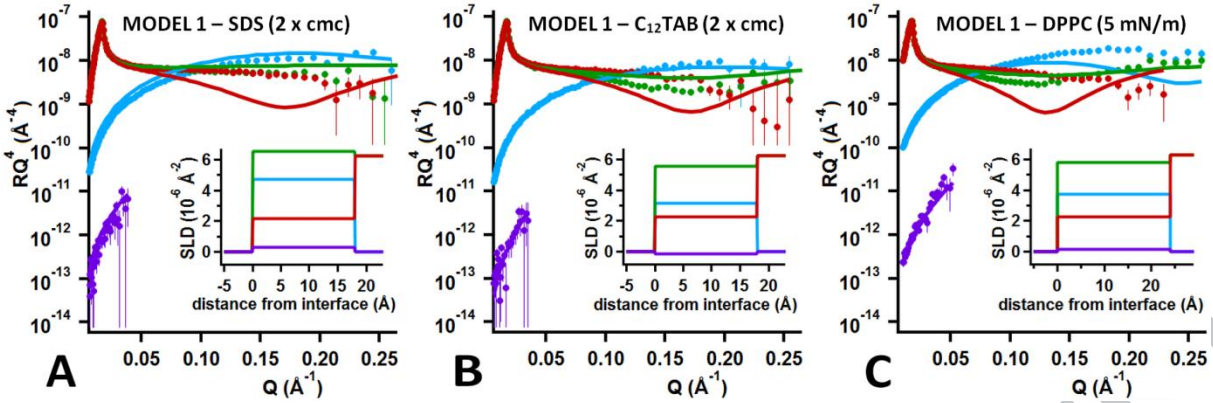

Figure 2. Neutron reflectivity data of monolayers of (A) SDS and (B) C_{12}TAB at 2 times their CMCs, and (C) DPPC at 5 mN m^{-1}, recorded in (blue) d-surf/ACMW, (green) d-surf/D_2O, (red) h-surf/D_2O and (purple) h-surf/ACMW: application of Model 1. The respective global χ^2 values for the 3 systems are 212, 86 and 371.

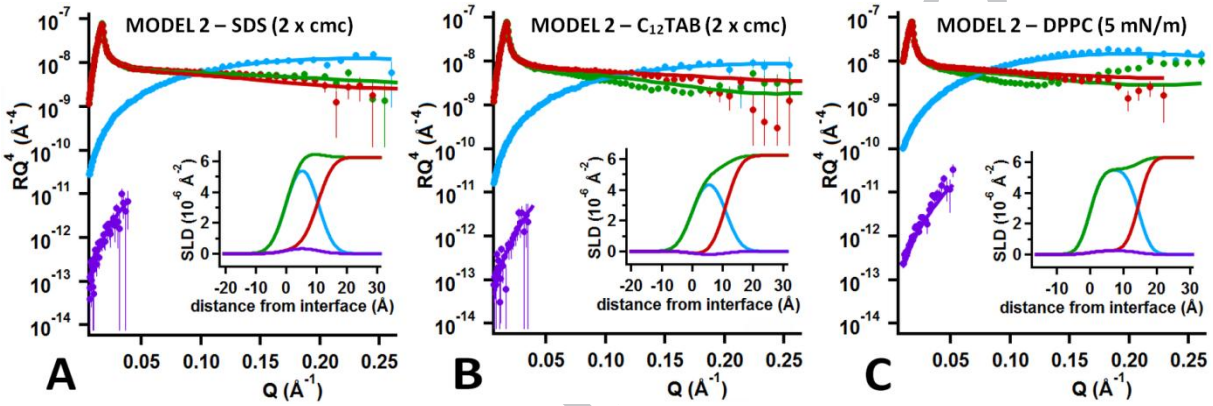

Figure 3. Neutron reflectivity data of (A) SDS and (B) C_{12}TAB at 2 times their CMCs, and (C) DPPC at 5 mN m^{-1} recorded in (blue) d-surf/ACMW, (green) d-surf/D_2O, (red) h-surf/D_2O and (purple) h-surf/ACMW: application of Model 2. The respective global χ^2 values for the 3 systems are 25, 39 and 74.

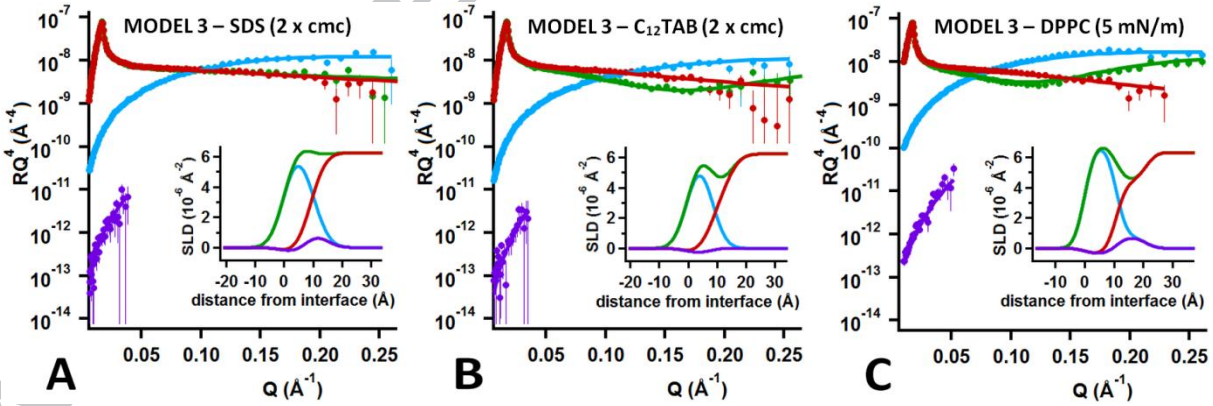

Figure 4. Neutron reflectivity data of monolayers of (A) SDS and (B) C_{12}TAB at 2 times their CMCs, and (C) DPPC at 5 mN m^{-1}, recorded in (blue) d-surf/ACMW, (green) d-surf/D_2O, (red) h-surf/D_2O and (purple) h-surf/ACMW: application of Model 3. The respective global χ^2 values for the 3 systems are 18, 30 and 13.

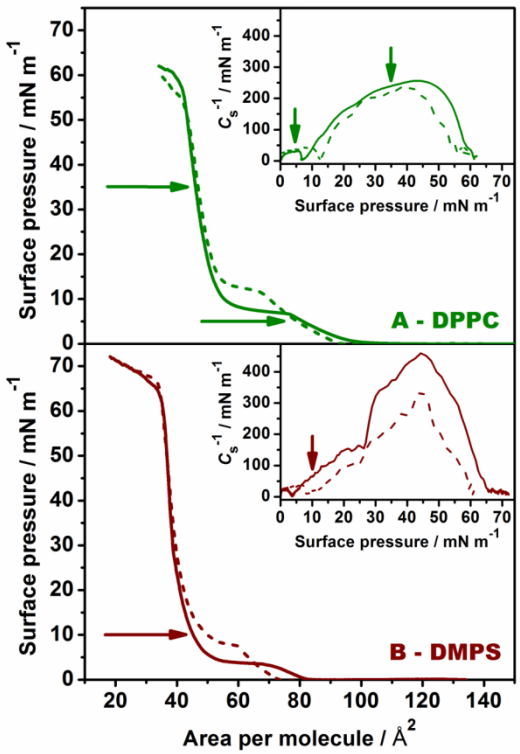

Figure 5. Surface pressure/area isotherms for hydrogenous (solid) and deuterated (dashed) monolayers of (A) DPPC and (B) DMPS. The inset shows corresponding data on the compression modulus as a function of the surface pressure. The arrows mark the phospholipid systems studied in the present work, i.e., DPPC at 5 and 35 mN m^{-1} and DMPS at 10 mN m^{-1}.

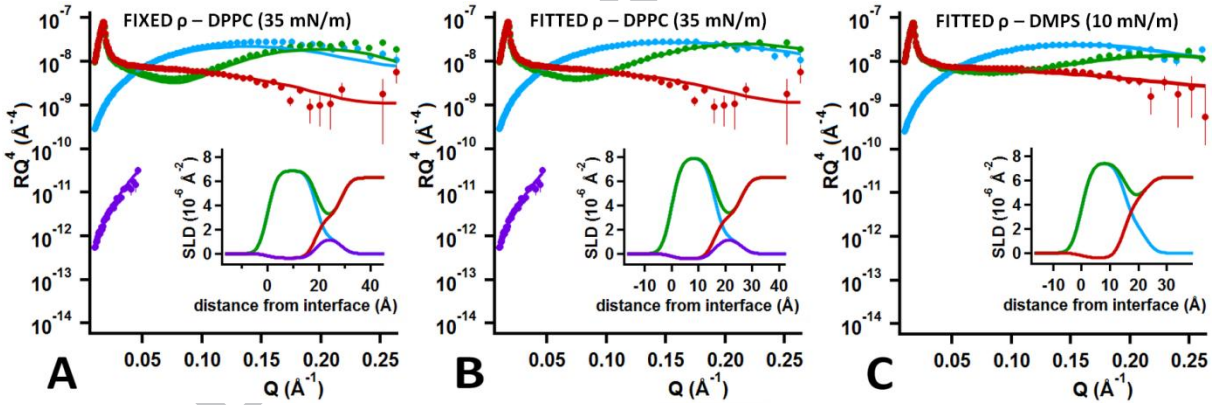

Figure 6. Neutron reflectivity data of monolayers of (A and B) DPPC at 35 mN m^{-1}, and (C) DMPS at 10 mN m^{-1}, recorded in (blue) d-surf/ACMW, (green) d-surf/D_2O, (red) h-surf/D_2O and (purple) h-surf/ACMW: (A) without and (B and C) with optimization of the scattering length density of layer 1 to account for compaction of the chains as a result of their phase: application of Model 3. Note that the h-DMPS/ACMW data were omitted from the data analysis because of reasons detailed in part 4 of the Supporting Information. The respective global χ^2 values in the first two panels are 85 and 20.

Graphical abstract